Kalman Filtering Sliding Mode Controller Design for Stabilizing and Trajectory Tracking of Inverted Pendulum

Akshaya Kumar Patra, Alok Kumar Mishra, Anuja Nanda, Lalit Mohan Satapathy, Amaresh Gantayet, Ramachandra Agrawal, and Abhishek Patra

Abstract The aim of this paper is to design a Kalman filtering sliding mode controller (KFSMC) for control of cart position (CP), and angular position (AP) of the pendulum under uncertainties and disturbances. For designing of the KFSMC, the fourth-order state-space model of the inverted pendulum (IP) is considered. In this control strategy, the conventional sliding mode controller (CSMC) is reformulated with a state estimator based on the Kalman filtering approach to improve the control performance. The validation of the improved control performance of KFSMC is established by comparative result investigation with other published control algorithms. The comparative results clearly reveal the better response of the proposed approach to control the system dynamics within a stable range with respect to accuracy, robustness, and ability to handle uncertainties.

Keywords Inverted pendulum · Angular displacement · Kalman filter · Sliding mode control

A. K. Patra (✉) · A. K. Mishra · A. Nanda · L. M. Satapathy · A. Gantayet · R. Agrawal · A. Patra
Department of EEE, Institute of Technical Education and Research, Siksha 'O' Anusandhan (Deemed to be University), Bhubaneswar 751030, India
e-mail: hiakp@yahoo.com

A. K. Mishra
e-mail: malok2010@gmail.com

A. Nanda
e-mail: anujananda@soa.ac.in

L. M. Satapathy
e-mail: lalitsatapati@soa.ac.in

A. Gantayet
e-mail: amareshgantayet@soa.ac.in

R. Agrawal
e-mail: ramachandra1agrawal@gmail.com

A. Patra
e-mail: pabhishek720@gmail.com

G. Pradhan et al. (eds.), *Advances in Electrical Control and Signal Systems*,
Lecture Notes in Electrical Engineering 665,
https://doi.org/10.1007/978-981-15-5262-5_28

1 Introduction

The control of IP is a standard problem among all other problems in the control system engineering field owing to non-minimum phase, nonlinear, and under-actuated characteristics as reported in the references [1–3]. Additionally, the IP system exhibits a significant number of industrial applications like self-balancing two-wheeled vehicles or a kind of Sag-way, guided missiles, rockets, intelligent robots, and other crane models [4]. In this present study, an adaptive law of control approach is being tested and analyzed to choose the IP system as it possesses a significant relevance with the control dynamics. During the past three decades, so many control strategy techniques are suggested and tested for control of AP of pendulum within the stable range. Time-discrete and switching PID control strategy is implemented in IP problems with variable control gains based on the measured AP of the pendulum [5, 6]. However, the optimal gain parameter setting, a lesser range of robust control, and need of change of gain setting with varying conditions are the major limitations to limit the real-time application of these controllers. Among other projected robust control algorithms implemented for limiting the AP of the pendulum are fuzzy [7], linear quadratic regulator (LQR) [8–10], neurocontrol [11], backstepping control [12], passivity control [13], state feedback control [14], H-infinity ($H\infty$) control [15], sliding mode (SM) control [16], fuzzy sliding mode (FSM) control [17, 18], and BLQG control [19]. However, even if these control techniques are implemented effectively to control the AP of the pendulum with better accuracy, still they fail to handle various constraints and random change found in a trajectory of motion in the pendulum. These control techniques are not completely insensitive to the disturbances and the uncertainties of the model in spite of the improved performance. Hence, optimal control parameters setting for better performance and for avoiding slow response following process disturbance, the current work suggests an alternative novel hybrid technique based on the Kalman filtering and sliding mode control concept.

In this study, a hybrid concept based on Kalman filtering approach and principles of sliding mode control is projected with the title Kalman filtering sliding mode controller (KFSMC). The hybrid approach concept leads to an enhanced control performance with respect to robustness, accuracy, stability, and better ability to handle uncertainty. The novel idea followed in this formulation is to modify CSMC with a state estimator according to the approach of Kalman filtering. Secondly, a stabilizing control law is framed by using the Kalman filtering approach [20–22]. Application of the proposed approach is to control the AP of pendulum results to ensure a better robust controller in comparison with other contemporary well-accepted methods under both harmonized and incompatible uncertainties.

The highlights of this manuscript are as follows:

- Development of a SIMULINK model of an IP.
- Design of a KFSMC to control the AP of the pendulum within a stable range.

- Estimation of the control actions of the KFSMC under huge deviation of process disturbance.
- Comparative investigation to certify the better response of the KFSMC.

This manuscript is structured as follows: Sect. 2 concisely illustrates the IP system with mathematical details reflecting to its dynamic characteristics. Also, it clearly demonstrates the simulation execution of the system on MATLAB environment. A detailed presentation on how the control technique is formulated and how it is implemented for this problem is presented in Sect. 3. Comparative results of the proposed approach with other published control techniques and the related analysis are provided in Sect. 4. The concluding comments are summarized in Sect. 5.

2 Problem Formulation and Modeling

2.1 System Overview

The closed-loop model of the IP is depicted in Fig. 1a. The applied horizontal force $F(t)$ and $v(t)$ are reflected as the process disturbance and the sensor noise, respectively, in this study. The controller receives information about the AP of the pendulum as an input to provide the optimal control force $u(t)$, and it balances the pendulum.

2.2 System Modeling

Figure 1b reflects the cart-pendulum model connected to a flexible cart rail with a free swinging pole. The CP is being controlled by a DC motor. The nonlinear IP modeling through the Newton's law-based mathematical equations has been carried out. It is presumed that the vertical force does not affect the CP and the CP is disturbed by the horizontal force $F(t)$ based on the operation of the DC motor [23, 24]. All the physical activities of the IP system are expressed mathematically and specified by Eqs. (1) and (2). All nomenclature and specifications for IP are shown in Tables 1 and 2, respectively. The SIMULINK model of the IP is established with respect to the Eqs. (1) and (2) as displayed in Fig. 1c.

$$(M+m)\frac{\mathrm{d}^2x(t)}{\mathrm{d}t^2} - ml\frac{\mathrm{d}^2\theta(t)}{\mathrm{d}t^2}\cos\theta(t) + ml\left(\frac{\mathrm{d}\theta(t)}{\mathrm{d}t}\right)^2\sin\theta(t) + b\frac{\mathrm{d}x(t)}{\mathrm{d}t} = F(t) \tag{1}$$

$$\left(i+Ml^2\right)\frac{\mathrm{d}^2\theta(t)}{\mathrm{d}t^2} - mgl\sin\theta(t) = ml\frac{\mathrm{d}^2x(t)}{\mathrm{d}t^2}\cos\theta(t) \tag{2}$$

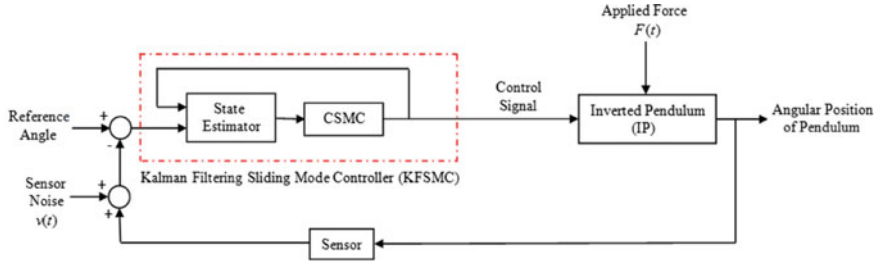

(a)

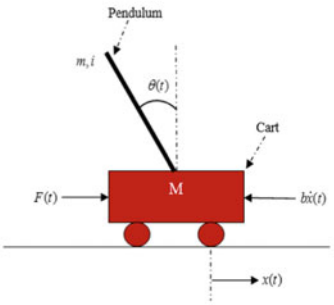

(b)

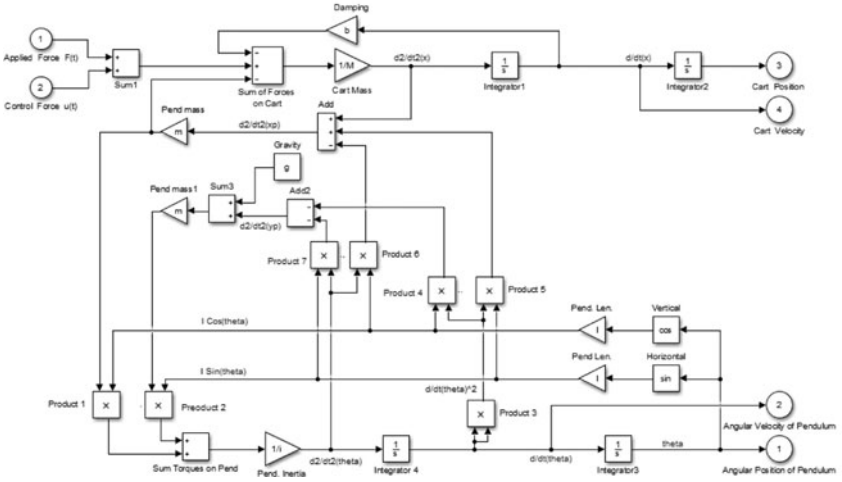

(c)

Fig. 1 **a** IP model with KFSMC; **b** schematic model of the IP system; **c** simulation model of the nonlinear IP system; **d** the horizontal force acting on the cart at the time of 0.1 s

Fig. 1 (continued)

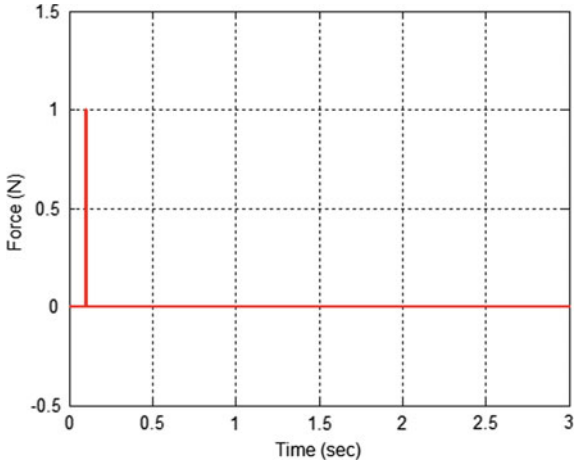

(d)

Table 1 IP model states and parameters

Symbol	Description
$F(t)$	Horizontal force acting on the cart
$b\frac{\mathrm{d}x(t)}{\mathrm{d}t}$	Frictional force acting on the cart
$x(t)$, $\frac{\mathrm{d}x(t)}{\mathrm{d}t}$, $\frac{\mathrm{d}^2x(t)}{\mathrm{d}t^2}$	Cart position, cart velocity, and cart acceleration, respectively
$\theta(t)$, $\frac{\mathrm{d}\theta(t)}{\mathrm{d}t}$, $\frac{\mathrm{d}^2\theta(t)}{\mathrm{d}t^2}$	AP, angular velocity, and angular acceleration of pendulum, respectively

Table 2 IP model specification values

Symbol	Physical meaning	Value
M	Cart mass	0.5 kg
m	Pendulum mass	0.2 kg
i	Inertia	0.3 kg m^2
g	Gravitational acceleration	9.8 $\mathrm{m/s}^2$
b	Frictional coefficient	0.1 N.s/m
l	Pendulum length	0.3 m

2.3 Linearization of IP Model

The nonlinear IP system is linearized surrounding the operating point for the design of KFSMC to control the system dynamics within the stable range. The linearization of the IP system based on Eqs. (1) and (2) is done by neglecting the higher-order terms such as $\left(\frac{\mathrm{d}\theta(t)}{\mathrm{d}t}\right)^2$. For linearization of the nonlinear IP system, the dynamic Eqs. (1) and (2) are reduced to Eqs. (3) and (4) based on the stable conditions such as $\theta(t) = 0$, $\frac{\mathrm{d}^2\theta(t)}{\mathrm{d}t^2} \cong 0$, and $\cos(0) = 1$.

$$(M+m)\frac{\mathrm{d}^2x(t)}{\mathrm{d}t^2}+b\frac{\mathrm{d}x(t)}{\mathrm{d}t}-ml\frac{\mathrm{d}^2\theta(t)}{\mathrm{d}t^2}=F(t) \tag{3}$$

$$\left(i+ml^2\right)\frac{\mathrm{d}^2\theta(t)}{\mathrm{d}t^2}-mgl\theta(t)=ml\frac{\mathrm{d}^2x(t)}{\mathrm{d}t^2} \tag{4}$$

The transfer function (TF) of the CP and AP of the pendulum is derived as follows [23]:

$$\frac{X(s)}{U(s)}=\frac{\frac{\left(i+ml^2\right)s^2-mgl}{\psi}}{s^4+\frac{b\left(i+ml^2\right)}{\psi}s^3-\frac{(M+m)mgl}{\psi}s^2-\frac{bmgl}{\psi}s} \tag{5}$$

$$\frac{\theta(s)}{U(s)}=\frac{\frac{ml}{\psi}s}{s^3+\frac{b\left(i+ml^2\right)}{\psi}s^2-\frac{(M+m)mgl}{\psi}s-\frac{bmgl}{\psi}} \tag{6}$$

where $\psi=\left[(M+m)\left(i+Ml^2\right)-ml^2\right]$. The linearized equation of the IP system with *F(t)* and *v(t)* based on the Eqs. (5) and (6) can be expressed as follows [23]:

$$\left.\begin{array}{l}\frac{\mathrm{d}x_m(t)}{dt}=\dot{x}_m(t)=A_mx_m(t)+B_mu(t)+B_dF(t)\\ y(t)=C_mx_m(t)+D_mu(t)+v(t)\end{array}\right\} \tag{7}$$

where $x_m(t)$, $u(t)$, and $y(t)$ are represented as the state variable, control input, and regulated output, respectively. The state-space matrices of the IP system are represented as A_m, B_m, C_m, D_m and B_d. The detailed description of linearization is described in the literature [23]. In MATLAB, the command *'linmod'* is used to evaluate the state-space matrices on the SIMULINK model of IP as depicted in Fig. 1c.

2.4 Response of IP Model

There are four roots in IP system. One of them lies in right-hand side of the complex plane. As a result, the system becomes unstable. This needs the design of an adaptive controller for improving the stability of the system by means of shifting the roots into the left-hand side of the complex plane. The IP system SIMULINK model in the open-loop form is depicted in Fig. 1c. The IP system consists of two inputs and four outputs. The control force $u(t)$ and applied horizontal force $F(t)$ are the two inputs of the IP system. The CP and AP of the pendulum are the four outputs of the IP system. An uncontrolled system dynamics such as AP of the pendulum and CP are being observed owing to the application of 1 N impulsive horizontal force $F(t)$ on the cart at the time $t = 1.0$ s.

The uncontrolled system dynamics are illustrated in Fig. 2a, b. Figure 2a, b illustrates the unstable dynamics under various model uncertainties and disturbances. The unstable dynamics can be reduced by applying the suitable control techniques.

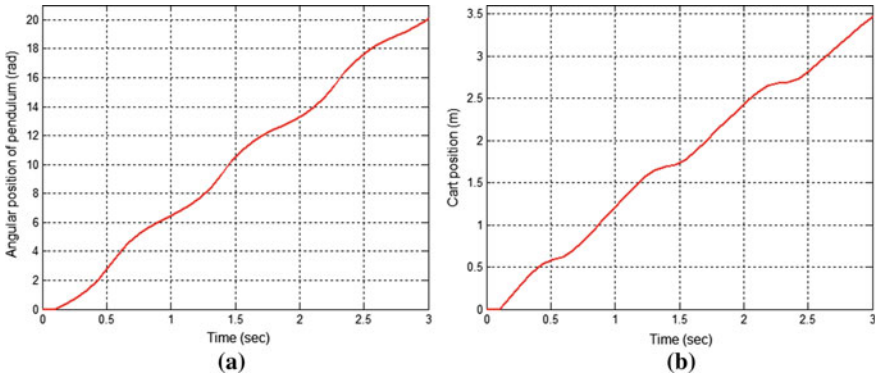

Fig. 2 **a** AP of pendulum with application of $F(t)$; **b** CP with application of $F(t)$

In this case, the AP of the pendulum is the most essential outcome that needs to be controlled within a stable range through suitable control techniques, and CP is analyzed in order to view the motion trajectory.

3 Control Algorithm

The KFSMC control algorithm is demonstrated in this section. The closed-loop system response with respect to robustness, accuracy, and stability are analyzed. The control specifications such as settling time t_s, steady-state error e_{ss}, maximum overshoot $O_{\max}$, and maximum undershoot $U_{\max}$ are also evaluated and examined with proper validation of the controller action.

3.1 Design of KFSMC

The linearized model of the IP as discussed in Sect. 2.3 has been taken for the formulation of the suggested control algorithm to regulate the CP and AP of the pendulum. For accomplishing an upgraded performance and the adjustment of controller parameters of the suggested KFSMC, it is integrated into the linearized model of the IP as illustrated in Fig. 3. The KFSMC is designed by integrating a state estimator with the CSMC as shown in Fig. 1a. The state estimator is implemented to estimate all the states of the system in a recursive manner to enhance the control performances such as robustness, accuracy, and stability. The linearized model of the IP with $F(t)$ and $v(t)$ is formulated as represented in Eq. (7), where both $v(t)$ and $F(t)$ are represented as the Gaussian noise. The relationship between $v(t)$ and $F(t)$ is as follows:

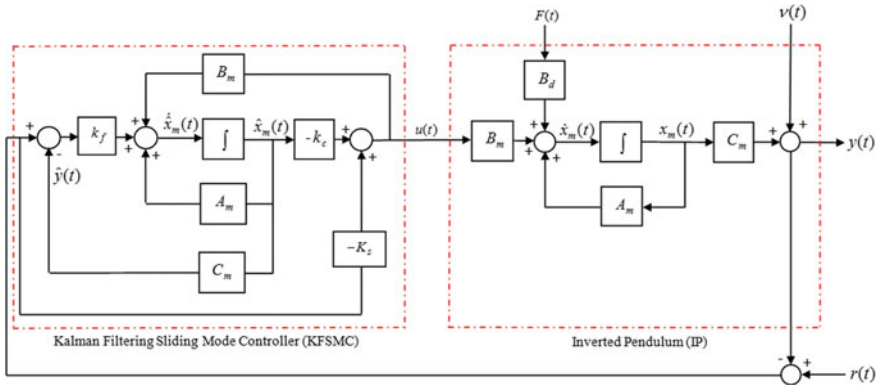

Fig. 3 Closed-loop IP model with KFSMC in the state-space representation

$$\left.\begin{aligned} E\{F(t)\} &= 0 \\ E\{v(t)\} &= 0 \end{aligned}\right\} \tag{8}$$

$$E\left\{F(t)F^T(\tau)\right\} = Q_2\delta(t-\tau) \tag{9}$$

$$E\left\{v(t)v^T(\tau)\right\} = R_2\delta(t-\tau) \tag{10}$$

$F(t)$ is uncorrelated to the $v(t)$; therefore, it can be defined as follows:

$$E\left\{F(t)v^T(\tau)\right\} = 0 \tag{11}$$

where Q_2 and R_2 are symbolized as the positive semi-definite intensity matrices of the $F(t)$ and $v(t)$, respectively. Figure 3 illustrates the linearized model of the IP with the feedback gain k_c and Kalman filtering gain k_f. The mathematical expressions of k_c and k_f are presented in Sect. 3.1.2. The calculation of the TF of the KFSMC is described in Sect. 3.1.3.

The control signal $u(t)$ of proposed controller has two major components such as switching function $u_{\text{st}}(t)$ and equivalent control input $u_{\text{eq}}(t)$. This is defined as represented in Eq. (12).

$$u(t) = u_{\text{st}}(t) + u_{\text{eq}}(t) \tag{12}$$

For the formulation of the proposed control algorithm, two basic steps are required. In the first step, the switching function $u_{\text{st}}(t)$ is to be ensured reaching condition by pulling the all states of a nominal model inside the boundary layer near the sliding hyperplanes; as a result, chattering is reduced and also robustness of a system is improved. In the second step, the desired $u_{\text{eq}}(t)$ is to be formulated in such a manner that accuracy, and stability of a system is enhanced. The design procedures of first and second steps of the KFSMC are analyzed in Sects. 3.1.1 and 3.1.2, respectively.

3.1.1 Reaching Condition (RC)

To achieve RC, all the states of the nominal model are to be inside the boundary layer near the sliding hyperplanes. Secondly, these states should remain inside the boundary layer after that [20]. The robustness of a model is enhanced by achieving the RC. Under this situation, the system dynamics are independent to the model uncertainty and disturbances. It can be possible through the sliding hyperplane parameter G_s.

(A) *Sliding hyperplane parameter*:

The sliding hyperplane parameter G_s for a system with α number of inputs is related to the equal number of α hyperplane vectors as follows [20]:

$$s_i(t) = g_i^T x_m(t) \tag{13}$$

$$s(t) = G_s x_m(t) \tag{14}$$

where $s(t)$ stands for $s_i(t)$, G_s stands for g_i^T, $s_i(t) = [s_1(t), s_2(t), s_3(t), \ldots, s_\alpha(t)]$, $s_i(t)$ is the ith hyperplane vector, $g_i^T = [g_1, g_2, g_3, \ldots, g_\alpha]^T$, g_i^T is the transpose of ith hyperplane parameter, α is the number of inputs of a system, and i varies from 1 to α. When $s_i(t) = 0$, α number of hyperplanes move through the origin in state-space as shown in Fig. 4. These hyperplanes are called as sliding hyperplanes.

Under the above condition, $s(t)$ and G_s are known as the sliding hyperplane vector and sliding hyperplane parameter of the IP model, respectively. Equation (14) can be rewritten as follows:

$$\dot{s}(t) = G_s \dot{x}_m(t) \tag{15}$$

The G_s is derived by using the similarity transformation controllable canonical form (STCCF) of an IP model. The STCCF of an IP model is defined as follows [20]:

$$\dot{q}(t) = \overline{A}_m q(t) + \overline{A}_m u(t) + \overline{A}_d w(t) \tag{16}$$

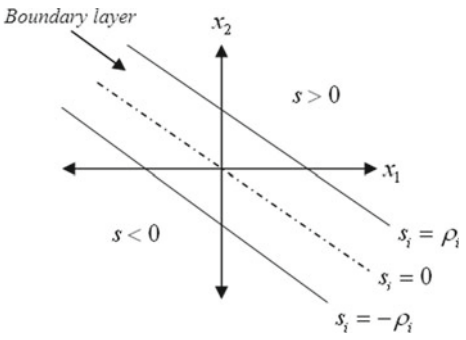

Fig. 4 Location of boundary layer near the sliding hyperplane

where $q(t) = Hx_m(t)$, $\overline{A}_m = HA_mH^{-1}$, $\overline{B}_m = HB_m$, $\overline{B}_d = HB_d$. The H matrix is computed by using Eq. (17).

$$H = \begin{bmatrix} F & B_m \end{bmatrix}^T \tag{17}$$

where $F = \text{null}\left(B_m^T\right)$. The $q(t)$ can be decomposed as follows:

$$q(t) = \begin{bmatrix} q_1(t) \\ q_2(t) \end{bmatrix} \tag{18}$$

where $q_1(t)$ and $q_2(t)$ are vectors with size of $(n-\alpha) \times \alpha$ and $\alpha \times \alpha$, respectively. The n represents the order of the A_m. When the rank of a system matrix A_m is not matched with the rank of the controllable matrix $c(A_m, B_m)$ of the system, the appropriate system is uncontrollable in nature. The system can be decomposed into controllable and uncontrollable parts. The decomposed controllable and uncontrollable parts of the system with respect to Eq. (16) are defined as follows [20]:

$$\begin{bmatrix} \dot{q}_1(t) \\ \dot{q}_2(t) \end{bmatrix} = \begin{bmatrix} \overline{A}_{m11} & \overline{A}_{m12} \\ \overline{A}_{m21} & \overline{A}_{m22} \end{bmatrix} \begin{bmatrix} q_1(t) \\ q_2(t) \end{bmatrix} + \begin{bmatrix} 0 \\ \overline{B}_{mr} \end{bmatrix} u(t) + \begin{bmatrix} 0 \\ \overline{B}_{dr} \end{bmatrix} w(t) \tag{19}$$

where $q_1(t)$ and $q_2(t)$ are the controllable and uncontrollable parts of the system, respectively. The $\overline{B}_{mr}$ consists of the last α-rows of the matrix $\overline{B}_m$, and $\overline{B}_{dr}$ consists of the last α-rows of the matrix $\overline{B}_d$. The sliding hyperplane vector can be expressed in the form of $q_1(t)$ and $q_2(t)$ as follows [20]:

$$s(t) = q_2(t) + kq_1(t) \tag{20}$$

The G_s can be derived based on Eqs. (14) and (20), as follows [20]:

$$G_s = \begin{bmatrix} k & I_\alpha \end{bmatrix} H \tag{21}$$

where k denotes the gain matrix of the proposed KFSMC, and I_α denotes an unitary matrix with dimension of $\alpha \times \alpha$.

(B) *Gain matrix of KFSMC*

The k is computed based on the IP model dynamics for the minimum value of the quadratic performance index j as specified in Eq. (22).

$$j = \int_0^\infty \left[q(t)^T Q_q q(t)\right] \mathrm{d}t \tag{22}$$

where $Q_q = \left(H^{-1}\right)^T Q_1 H^{-1}$ and $Q_1 = C_m^T C_m$. The Q_1 signifies a positive semi-definite weighted matrix of state. The matrix Q_q can be decomposed with respect to

Eq. (19) as follows:

$$Q_q = \begin{bmatrix} Q_r & N \\ N^T & R_1 \end{bmatrix} \tag{23}$$

where the matrix Q_r is the first subpart of the matrix Q_q with size of $(n-\alpha) \times (n-\alpha)$. The matrix N is the second subpart of the matrix Q_q with size of $(n-\alpha) \times \alpha$. The N^T is the third subpart of the Q_q with dimension of $\alpha \times (n-\alpha)$. The R_1 symbolizes a positive definite weighted matrix of input, and it is the fourth subpart of the matrix Q_q with size of $\alpha \times \alpha$. Equation (22) can be reformulated as follows:

$$j = \int_0^\infty \left[q_1(t)^T Q_r q_1(t) + 2q_1(t)^T N q_2(t) + q_2(t)^T R_1 q_2(t) \right] \mathrm{d}t \tag{24}$$

The system can achieve RC, only when $s(t) = 0$. Under RC, the system dynamics can be formulated based on the full state feedback along with size of $(n-\alpha) \times \alpha$ as follows [20]:

$$\dot{q}_1(t) = \overline{A}_{m1} q_1(t) + \overline{A}_{m12} q_2(t) \tag{25}$$

The k is computed based on the Eqs. (23) and (25) for the minimum value of the quadratic performance index as specified in Eq. (26).

$$k = R_1^{-1} \left(\overline{A}_{m12}^T P + N^T \right) \tag{26}$$

where P denotes the controller algebraic Riccati equation (CARE) solution. The CARE is specified as follows [20]:

$$\begin{aligned} &P(\overline{A}_{m11} - \overline{A}_{m12} R_1^{-1} N^T) + (\overline{A}_{m11}^T - N R_1^{-1} \overline{A}_{m12}^T) P \\ &- P \bar{A}_{m12} R_1^{-1} \overline{A}_{m12}^T P + Q_r - N R_1^{-1} N^T = 0 \end{aligned} \tag{27}$$

The sliding hyperplane parameter G_s can be computed by putting Eq. (26) in Eq. (21). The system can achieve RC and enhanced robustness through the sliding hyperplane parameter G_s. To satisfy the RC and chattering free control is chosen as [20]:

$$u(t) = -(G_s B_m)^{-1} \mathrm{diag}(\eta) \mathrm{sat}(s(t)) + u_{\mathrm{eq}}(t) \tag{28}$$

where $-(G_s B_m)^{-1} \mathrm{diag}(\eta) \mathrm{sat}(s(t))$ is the switching function $u_{st}(t)$ and $\mathrm{diag}(\eta)$ is a diagonal matrix with ith diagonal element equal to a positive number η_i. The ith element of $\mathrm{sat}(s(t))$ is formulated as:

$$\text{sat}(s_i(t)) = \begin{cases} \text{sgn}(s_i(t)) & \text{if } |s_i(t)| > \rho_i \\ s_i/\rho_i & \text{otherwise} \end{cases} \tag{29}$$

where ρ_i denotes the boundary layer thickness nearby the ith hyperplane as shown in Fig. 4.

3.1.2 Equivalent Control Input $u_{\text{eq}}(t)$

To satisfy the RC, the $u_{\text{eq}}(t)$ can be formulated with the use of k_f and k_c. The states of the system are estimated recursively based on the Kalman filtering approach to enhance the system response. The estimated state-space equation of the system is defined as [20]:

$$\dot{\hat{x}}_m(t) = A_m\hat{x}_m(t) + B_m u(t) + k_f[r(t) - y(t) - \hat{y}(t)] \tag{30}$$

$$\hat{y}(t) = C_m\hat{x}_m(t) \tag{31}$$

where $\hat{x}_m(t)$ signifies the estimated state and $\hat{y}(t)$ signifies the estimated output.

The k_f can be formulated as [20]:

$$k_f = \Sigma_k C_m^T R_2^{-1} \tag{32}$$

where Σ_k signifies the filter algebraic Riccati equation (FARE) solution. The FARE is specified as follows [20]:

$$A_m\Sigma_k + \Sigma_k A_m^T + B_d Q_2 B_d^T - \Sigma_k C_m^T R_2^{-1} C_m \Sigma_k = 0 \tag{33}$$

The sliding hyperplane vector $s(t)$ can be formulated with the use of G_s and $\hat{x}_m(t)$ as follows [20]:

$$s(t) = G_s\hat{x}_m(t) \tag{34}$$

To satisfy the RC, the $u_{\text{eq}}(t)$ can be derived from Eqs. (30) and (34) as [20]:

$$u_{\text{eq}}(t) = -(G_s B_m)^{-1}\left[G_s\left(A_m - k_f C_m\right)\hat{x}_m(t) + G_s k_f[r(t) - y(t)]\right] \tag{35}$$

Under RC, the control law $u(t)$ of suggested KFSMC is formulated based on Eqs. (28), (29), and (35) as follows [20]:

$$u(t) = -(G_s B_m)^{-1}\left[G_s\left(A_m - k_f C_m + \gamma I_n\right)\hat{x}_m(t) + G_s k_f[r(t) - y(t)]\right] \tag{36}$$

$$u(t) = -k_c\hat{x}_m(t) - K_s[r(t) - y(t)] \tag{37}$$

Table 3 The optimal values of control parameters

Q_1	R_1	Q_2	R_2
$1000 * C_m^T * C_m$	1	0.01	0.0025

where $K_s = (G_s B_m)^{-1} G_s k_f$ and $k_c = (G_s B_m)^{-1} G_s \left(A_m - k_f C_m + \gamma I_n\right)$. The I_n is an unitary matrix with size of $n \times n$, and n is the order of the A_m. The k_c and γ are denoted for the feedback gain and sliding parameter of the suggested KFSMC, respectively. The γ can be estimated as:

$$\gamma = \frac{\eta_i}{\rho_i} = \frac{\eta}{\rho} \tag{38}$$

where ρ_i and η_i are denoted for the thickness of the boundary layer and any positive number of the ith sliding hyperplane, respectively, as illustrated in Fig. 4. Both η_i and ρ_i are taken as identical value for each γ and set to η and ρ, respectively.

3.1.3 Transfer Function (TF) of KFSMC

The TF of the KFSMC is defined from Eqs. (30) and (37) as follows [20]:

$$K(s) = \beta_1 \left(s I_n - A_m + B_m \beta_1 + k_f C_m\right)^{-1} \beta_2 + (G_s B_m)^{-1} G_s k_f \tag{39}$$

where $K(s)$ is denoted as the TF of KFSMC, $\beta_1 = (G_s B_m)^{-1} G_s \left(A_m + \gamma I_n - k_f C_m\right)$ and $\beta_2 = k_f - B_m (G_s B_m)^{-1} G_s k_f$. The packed matrix notation of $K(s)$ is specified as follows [20]:

$$K(s) = \left[\begin{array}{c|c} A_m - B_m (G_s B_m)^{-1} G_s (A_m - k_f C_m + \gamma I_n) - k_f C_m & -B_m (G_s B_m)^{-1} G_s k_f + k_f \\ \hline -(G_s B_m)^{-1} G_s (A_m - k_f C_m + \gamma I_n) & -(G_s B_m)^{-1} G_s k_f \end{array}\right] \tag{40}$$

For the design of suggested KFSMC, the optimal values of control parameters are evaluated with help of MATLAB and represented as in Table 3.

4 Outcomes and Discussions

The response of the closed-loop IP with proposed KFSMC is described in detail in this section. The proposed control approach (KFSMC) is compared with other popular control algorithms to justify its enhanced performance.

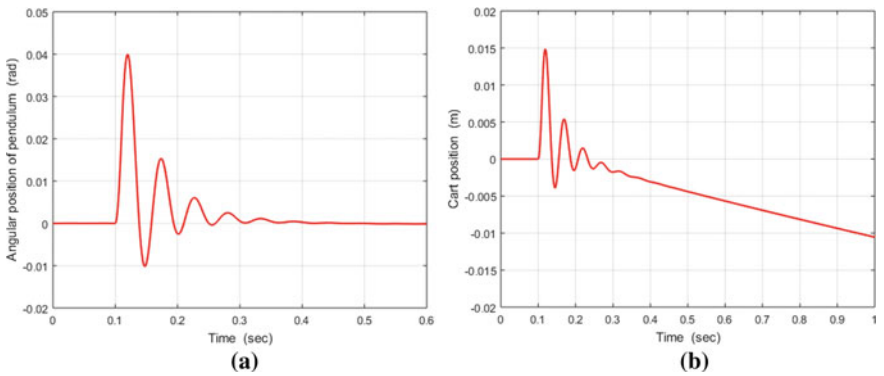

Fig. 5 **a** AP of the pendulum with the application of $F(t)$ based on KFSMC; **b** CP with the application of $F(t)$ based on KFSMC

4.1 Performance Analysis of IP System with KFSMC

In this section, all physical activities of the closed-loop IP model with suggested KFSMC are examined under different conditions and the huge deviation of applied horizontal force. The closed-loop system dynamics with 1 N impulsive horizontal force $F(t)$ at the time of 1.0 s are displayed in Fig. 5a, b. The outcomes clearly specify the pendulum achieves the zero AP with less settling time and cart also attains the balance position where the IP system is absolutely steady. To achieve the enhanced system response, the required control force $u(t)$ is generated by the suggested KFSMC and demonstrated in Fig. 6.

4.2 Robustness of the KFSMC

Figure 7 illustrates the AP and AV of the pendulum with suggested KFSMC under the huge deviation of applied horizontal force $F(t)$. The time-domain outcomes under huge deviation of applied forces show the enhanced performance of the closed-loop IP model with KFSMC. Overall in each case, the pendulum achieves finally zero AP and zero AV with less settling time. As indicated by the results, the suggested KFSMC robust performance under the huge deviation of applied horizontal forces is much better.

4.3 Stability Investigation

Figure 8a, b illustrates the magnitude plots result of the open-loop and closed-loop IP system to verify and analyze the stability conditions. From both the magnitude

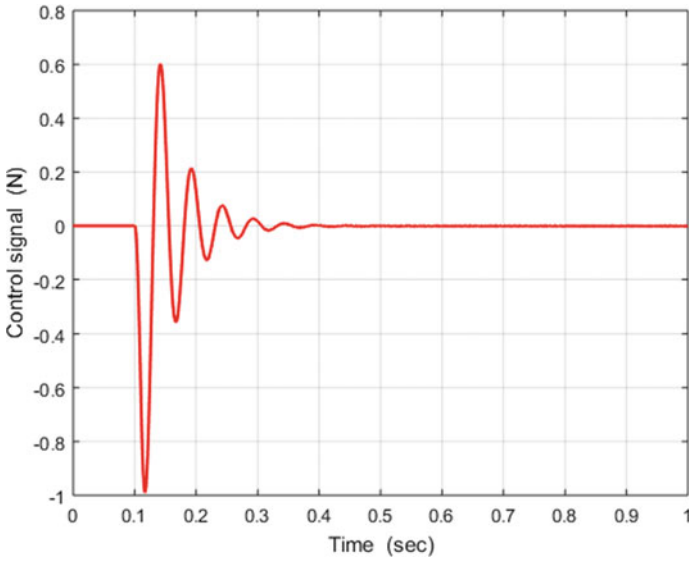

Fig. 6 Controlled signal $u(t)$ of the KFSMC

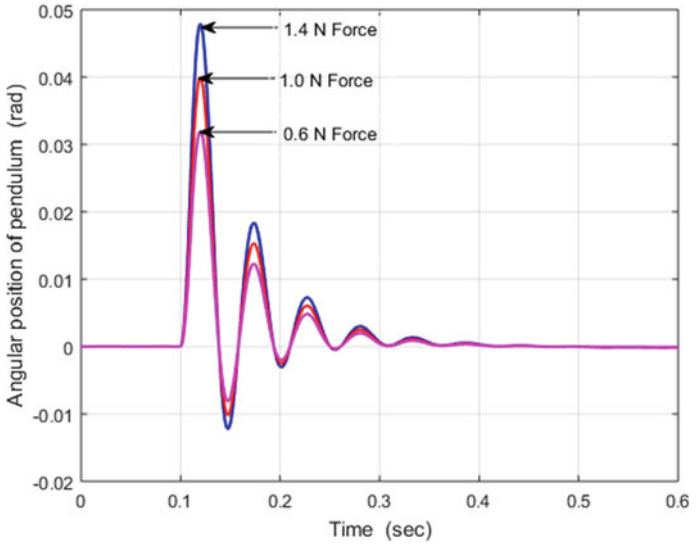

Fig. 7 AP of the pendulum with a deviation of $\pm 40\%$ applied $F(t)$ based on KFSMC

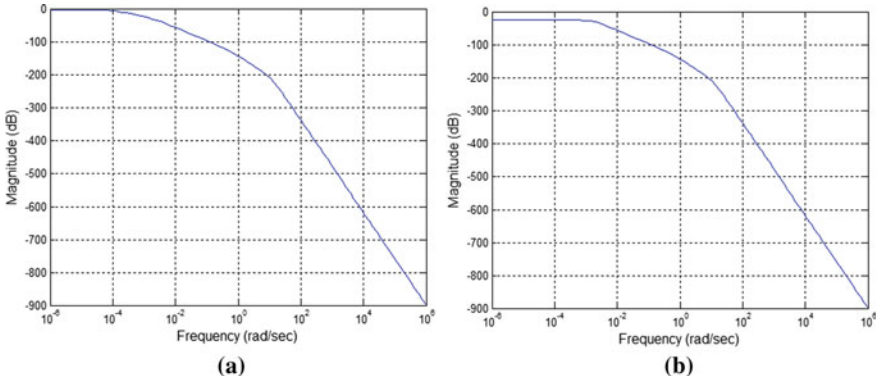

Fig. 8 **a** Magnitude plot of the IP system; **b** Magnitude plot of the closed-loop IP system

plots, it is observed a better smoothness referring to the wider steady-state stability of closed-loop system (Fig. 8b) than the open-loop system (Fig. 8a). In other words, the bandwidth is increased in case of a closed-loop system with KFSMC than the open-loop system. This clearly indicates a faster dynamics, and also it results zero AP and zero AV of pendulum with quick settling time in case of the closed-loop system. This justifies better stability during system operation.

4.4 Comparative Study

The proposed KFSMC control approach is compared with other popular control approaches such as PID, fuzzy, LQR, $H\infty$, FSM, and BLQG which justify its enhanced performance as a controller. Figure 5a illustrates the effect of applied force in the AP of the pendulum with the proposed KFSMC approach. Table 4 presents a comparative analysis with respect to t_s (sec), O_{Max} (rad), U_{Max} (rad), noise (%), and

Table 4 Comparative result analysis related to AP of pendulum

Controller	PID [5]	Fuzzy [7]	LQR [9]	$H\infty$ [15]	FSM [18]	BLQG [19]	KFSMC (proposed)
Applied force (N)	1	1	1	1	1	1	1
t_s (s)	2.8	3.0	3.2	1.5	1.6	0.4	0.36
O_{Max} (rad)	0.1	0.226	0.081	0.107	0.042	0.041	0.04
U_{Maz}(rad)	0.01	0.087	0.02	0.045	0.151	0.01	0.009
Noise (%)	10	10	5	5	5	1	1
e_{ss}(%)	0	0	0	0	0	0	0

$e_{ss}(\%)$. The effect of applied force in the AP of pendulum applying different control approaches such as PID, fuzzy, LQR, $H\infty$, FSM, and BLQG is also demonstrated in Table 4 based on the references [5, 7, 9, 15, 18, 19], respectively. Similar working conditions are followed with the same level of sensor noise in all control techniques application for comparison.

The AP of pendulum under 1 N impulsive horizontal force is tested. The corresponding results are presented for the various control approaches along with the proposed KFSMC with respect to time-domain specifications such as O_{Max}(rad), U_{Max}(rad), and t_s(s). The results signify the better controllability of the KFSMC. The simulation results also demonstrate the high noise and chattering elimination capability with high robustness for the proposed approach. Overall, by looking to the above comparative analysis, the findings of suggested approach advantages are the higher accuracy and stability, more robustness, high noise and chattering elimination capability, and better capability to handle uncertainty under various conditions and huge deviation of road disturbance.

5 Conclusions

The manuscript proposed a novel control strategy (KFSMC) based on the Kalman filtering approach to balance the pendulum. To justify its enhanced performance, it has been applied and tested to control the system dynamics of IP system within the stable range. Initially, the IP system is modeled as the fourth-order state-space representation. Then, the proposed control approach (KFSMC) is designed. In suggested KFSMC, state estimator is utilized to enhance the control performance. The comparative results clearly reflect that the suggested KFSMC is arrived at better performance than the other control approaches such as PID, fuzzy, LQR, $H\infty$, FSM, and BLQG with respect to stability, reliability, and robustness under various abnormal conditions and disturbances. The better performance of the suggested approach in terms of improved accuracy and stability, enhanced robustness, high noise and chattering elimination capability, and better ability to control uncertainty which justifies its real-time application.

References

1. Iqbal, J., Islam, R.U., Syed, Z.A., Abdul, A.K., Ajwad, S.A.: Automating industrial tasks through mechatronic systems—a review of robotics in industrial perspective. Tehnicki vjesnik Tech. Gaz. **23**, 917–924 (2016)
2. Ajwad, S.A., Asim, N., Islam, R.U., Iqbal, J.: Role and review of educational robotic platforms in preparing engineers for industry. Maejo Int. J. Sci. Technol. **11**, 17–34 (2017)
3. Bettayeb, M., Boussalem, C., Mansouri, R., Al-Saggaf, U.: Stabilization of an inverted pendulum-cart system by fractional PI-state feedback. ISA Trans. **53**, 508–516 (2014)

4. Iqbal, J., Ullah, M., Khan, S.G., Khelifa, B., Ukovic, S.C.: Nonlinear control systems—a brief overview of historical and recent advances. Nonlinear Eng. **6**, 301–312 (2017)
5. Ghosh, A., Krishnan, T., Subudhi, B.: Brief paper—robust proportional-integral-derivative compensation of an inverted Cart-Pendulum System: an experimental study. IET Control Theory Appl. **6**(8), 1145–1152 (2012)
6. Wang, C., Yin, G., Liu, C., Fu, W.: Design and simulation of inverted pendulum system based on the fractional PID controller. In: IEEE 11th Conference on Industrial Electronics and Applications (ICIEA), pp. 1760–1764 (2016)
7. Magana, M.E., Holzapfel, F.: Fuzzy-logic control of an inverted pendulum with vision feedback. IEEE Trans. Educ. **41**(2), 165–170 (1998)
8. Ozana, S., Pies, M., Slanina, Z., Hajovsky, R.: Design and implementation of LQR controller for inverted pendulum by use of REX control system. In: IEEE International Conference on Circuits and Systems, vol. 1, pp. 343–347 (2012)
9. Kumar, E.V., Jerome, J.: Robust LQR controller design for stabilizing and trajectory tracking of inverted pendulum. Procedia Eng. **64**, 169–178 (2013)
10. Prasad, L.B., Tyagi, B., Gupta, H.O.: Modelling and simulation for optimal control of nonlinear inverted pendulum dynamical system using PID controller and LQR. In: Sixth Asia Modelling Symposium (Ams), 138–143 (2012)
11. Pasemann, F.: Evolving neurocontrollers for balancing an inverted pendulum. Netw. Comput. Neural Syst. **9**, 1–4 (1998)
12. Deng, L., Gao, S.: The design for the controller of the linear inverted pendulum based on backstepping. In: International Conference on Electronic and Mechanical Engineering and Information technology (EMEIT), vol. 6, pp. 2892–2895 (2011)
13. Jörgl, M., Schlacher, K., Gattringer, H.: Passivity based control of a cart with inverted pendulum. Appl. Mech. Mater. **332**, 339–344 (2013)
14. Žilić, T., Pavković, D.: Modeling and control of a pneumatically actuated inverted pendulum. ISA Trans. **48**, 327–335 (2009)
15. Lambrecht, P., Vander, G.: H-infinity control of an experimental inverted pendulum with dry friction. IEEE Contr. Syst. Mag. **13**(4), 44–50 (1988)
16. Wai, R.J., Chang, L.J.: Adaptive stabilizing and tracking control for a nonlinear inverted-pendulum system via sliding-mode technique. IEEE Trans. Ind. Electron. **53**, 674–692 (2006)
17. Tao, C.W., Taur, J., Chang, J.: Adaptive fuzzy switched swing-up and sliding control for the double-pendulum-and-cart system. IEEE Trans. Syst. Man Cybern. B Cybern. **40**(1), 241–252 (2010)
18. Chen, C.S., Chen, W.L.: Robust adaptive sliding-mode control using fuzzy modelling for an inverted-pendulum system. IEEE Trans. Ind. Electron. **45**(2), 297–306 (1998)
19. Patra, A.K., Rout, P.K.: Backstepping linear quadratic gaussian controller design for balancing an inverted pendulum. IETE J. Res. pp. 1–15 (2019)
20. Khalil, H.K.: (2002) Nonlinear Systems, 3rd edn. Prentice Hall, Upper Saddle River, New Jersey
21. Patra, A.K., Rout, P.K.: Adaptive sliding mode gaussian controller for artificial pancreas in TIDM patient. J. Process Control **58**, 23–27 (2017)
22. Patra, A.K., Rout, P.K.: Backstepping sliding mode Gaussian insulin injection control for blood glucose regulation in TIDM patient. J. Dyn. Sys., Meas., Control. **140** (9), 091006–091006-15 (2018)
23. Irfan, S., Mehmood, A., Razzaq, M.T., Iqbal, J.: Advanced sliding mode control techniques for inverted pendulum: modelling and simulation. Eng. Sci. Tech. Int. J (2018). https://doi.org/10.1016/j.jestch.2018.06.010
24. Ronquillo-Lomeli, G., Ríos-Moreno, G.J.: Nonnlinear identification of inverted pendulum system using volterra polynomials. Mech. Based Des. Struct. Mach **44**(1), 5–15 (2016)